

1 **Early epidemiological assessment of the transmission**
2 **potential and virulence of coronavirus disease 2019**
3 **(COVID-19) in Wuhan City: China, January-February,**
4 **2020**

5 **Authors:** Kenji Mizumoto^{1,2,3} §, Katsushi Kagaya⁴, Gerardo Chowell³

6 **Affiliations:**

7 ¹ Graduate School of Advanced Integrated Studies in Human Survivability, Kyoto
8 University Yoshida–Nakaadachi–cho, Sakyo–ku, Kyoto, Japan

9 ² Hakubi Center for Advanced Research, Kyoto University, Yoshidahonmachi,
10 Sakyo–ku, Kyoto, Japan;

11 ³ Department of Population Health Sciences, School of Public Health, Georgia State
12 University, Atlanta, Georgia, USA

13 ⁴ Center for Education and Research in Information Science and Technology (CERIST),
14 Graduate School of Information Science and Technology, The University of Tokyo,
15 Tokyo, Japan

16

17 §Corresponding author

18 Email addresses:

19 KM: mizumoto.kenji.5a@kyoto-u.ac.jp, KK: kagaya.katsushi.8e@kyoto-u.ac.jp,

20 GC: gchowell@gsu.edu

21 **Article type:**

22 Original Research

23 **Word count:**

24 Abstract: 347 (Max 350)

25 Main: 3103

26 **Abstract**

27 **Background:**

28 Since the first cluster of cases was identified in Wuhan City, China, in December, 2019,
29 coronavirus disease 2019 (COVID-19) rapidly spread around the world. Despite the
30 scarcity of publicly available data, scientists around the world have made strides in
31 estimating the magnitude of the epidemic, the basic reproduction number, and
32 transmission patterns. Accumulating evidence suggests that a substantial fraction of the
33 infected individuals with the novel coronavirus show little if any symptoms, which
34 highlights the need to reassess the transmission potential of this emerging disease. In
35 this study, we derive estimates of the transmissibility and virulence of COVID-19 in
36 Wuhan City, China, by reconstructing the underlying transmission dynamics using
37 multiple data sources.

38 **Methods:**

39 We employ statistical methods and publicly available epidemiological datasets to jointly
40 derive estimates of transmissibility and severity associated with the novel coronavirus.
41 For this purpose, the daily series of laboratory–confirmed COVID-19 cases and deaths
42 in Wuhan City together with epidemiological data of Japanese repatriated from Wuhan
43 City on board government–chartered flights were integrated into our analysis.

44 **Results:**

45 Our posterior estimates of basic reproduction number (R) in Wuhan City, China in
46 2019–2020 reached values at 3.49 (95%CrI: 3.39–3.62) with a mean serial interval of
47 6.0 days, and the enhanced public health intervention after January 23rd in 2020 was
48 associated with a significantly reduced R at 0.84 (95%CrI: 0.81–0.88), with the total
49 number of infections (i.e. cumulative infections) estimated at 1906634 (95%CrI:
50 1373500– 2651124) in Wuhan City, elevating the overall proportion of infected
51 individuals to 19.1% (95%CrI: 13.5–26.6%). We also estimated the most recent crude
52 infection fatality ratio (IFR) and time–delay adjusted IFR at 0.04% (95% CrI:
53 0.03%–0.06%) and 0.12% (95%CrI: 0.08–0.17%), respectively, estimates that are
54 several orders of magnitude smaller than the crude CFR estimated at 4.06%

55 **Conclusions:**

56 We have estimated key epidemiological parameters of the transmissibility and virulence
57 of COVID-19 in Wuhan, China during January-February, 2020 using an ecological
58 modelling approach. The power of this approach lies in the ability to infer
59 epidemiological parameters with quantified uncertainty from partial observations
60 collected by surveillance systems.

61 **Keywords:** epidemic; transmissibility; mathematical model; COVID-19; China

62

63 **Background**

64 The novel coronavirus (Severe acute respiratory syndrome coronavirus 2;
65 SARS-CoV-2) that erupted from China is a deadly respiratory pathogen that belongs to
66 the same family as the coronavirus responsible for the 2002-2003 Severe Acute
67 Respiratory Syndrome (SARS) outbreaks [1]. Since the first cluster of cases was
68 identified in Wuhan City, China, in December, 2019, the novel coronavirus disease 2019
69 (COVID-19) continues its relentless march around the world as of May 12nd, 2020 [2].
70 Nevertheless, China was hit hard by this emerging infectious disease, especially the city
71 of Wuhan in Hubei Province, where the first cluster of severe pneumonia caused by the
72 novel virus was identified. Meanwhile, the cumulative number of laboratory and
73 clinically confirmed cases and deaths in mainland China has reached 82918 and 4633,
74 respectively, as of May 10th, 2020 [3].

75 Because the morbidity and mortality burden associated with the novel
76 coronavirus has disproportionately affected the city of Wuhan, the center of the epidemic
77 in China, the central government of the People's Republic of China imposed a lockdown
78 and social distancing measures in this city and surrounding areas starting on January
79 23rd 2020. Indeed, out of the 82918 COVID-19 cases reported in China, 50339 cases
80 (60.7%) are from Wuhan City. In terms of the death count, a total of 3869 deaths
81 (83.5%) have been recorded in Wuhan city out of the 4633 deaths reported throughout
82 China. To guide the effectiveness of interventions, it is crucial to gauge the uncertainty
83 relating to key epidemiological parameters characterizing the transmissibility and the
84 severity of the disease. Despite the scarcity of publicly available data, scientists around
85 the world have made strides in estimating the magnitude of the epidemic, the basic
86 reproduction number, and transmission patterns [4-5]. Moreover, accumulating evidence

87 suggests that a substantial fraction of the infected individuals with the novel coronavirus
88 show little if any symptoms, which suggest the need to reassess the transmission
89 potential of this emerging disease [6]. For this purpose, in this study we employ
90 statistical methods and publicly available epidemiological datasets to jointly derive
91 estimates of transmissibility and severity associated with the novel coronavirus.

92

93 **Methods**

94 **Epidemiological data**

95 We linked our model to two different datasets. First, the daily series of
96 laboratory–confirmed COVID-19 cases and deaths in Wuhan City were extracted
97 according to date of symptoms onset or reporting date from several sources [3, 7-8].
98 Our analysis relies on epidemiological data reported prior to February 11th, 2020
99 because of the change in case definition that was announced on February 12th, 2020 [9].
100 As of February 11th, 2020, a total of 19559 confirmed cases including 820 deaths were
101 reported in Wuhan City. Second, epidemiological data of Japanese evacuees from
102 Wuhan City on board government–chartered flights were obtained from the Japanese
103 government. After arriving in Japan, all of the Japanese evacuees were kept in isolation
104 for about 14 days and examined for infection using polymerase chain reaction (PCR)
105 tests [7]. As of February 11th, a total of four flights with the Japanese evacuees left
106 Wuhan City. We collected information on the timing of the evacuee fights that left
107 Wuhan City as well as the number of passengers that tested positive for COVID-19 in
108 order to calibrate our model (Table S1).

109

110 **Statistical analysis**

111 Using the following integral equation model, we estimate the reproduction
112 number of COVID-19. Here, infected and reported cases are denoted by i and c ,
113 respectively.

114 We connected the daily incidence series with a discrete-time integral equation
115 to describe the epidemic dynamics. Let g_s denote the probability mass function of the
116 serial interval, e.g., the time from illness onset in a primary case to illness onset in the
117 secondary case, of length s days, which is given by

$$g_s = G(s) - G(s - 1) ,$$

118 For $s > 0$ where $G(\cdot)$ represents the cumulative distribution function of the gamma
119 distribution. Mathematically, we describe the expected number of new cases with day t ,
120 $E[c(t)]$ as follows,

$$E[c(t)] = \sum_{s=1}^{\infty} E[c(t-s)]R,$$

121 where $E[c(t)]$ represents the expected number of new cases with onset day t , where R
122 represents the average number of secondary cases per case.

123 Subsequently, we also employed the time-dependent variation in R to estimate
124 the impact of enhanced interventions on the reproduction number. This time dependence
125 was modelled by introducing a parameter δ_t , which is given by

$$\delta_t = \begin{cases} 1 & \text{otherwise} \\ \beta_1 & \text{if } t = \text{period}_1 \\ \beta_2 & \text{if } t = \text{period}_2 \end{cases}$$

126 where period_1 and period_2 represent the corresponding period from January 23rd to
127 February 2nd 2020 and from February 3rd to February 11th, 2020, respectively. January
128 23rd 2020 is the date when the central government of the People's Republic of China

129 imposed a lockdown in Wuhan and other cities in Hubei in an effort to quarantine the
 130 epicentre of the coronavirus (COVID-19) to mitigate transmission. Furthermore, we
 131 evenly divide the interval into two periods to incorporate the time-dependent effects on
 132 R using the parameters β_1 and β_2 which scale the effects of the intervention, taking
 133 values smaller than 1 [10].

134 To account for the probability of occurrence, θ [11], we assume that the number
 135 of observed cases on day t , $h(t)$, occurred according to a Bernoulli sampling process,
 136 with the expected values $E(c_i; H_{t-1})$, where $E(c_i; H_{t-1})$ denotes the conditional expected
 137 incidence on day t , given the history of observed data from day 1 to day $(t-1)$, denoted
 138 by H_{t-1} . Thus, the number of expected newly observed cases is written as follows:

$$E[h(t); H_{t-1}] = \begin{cases} (1 - \theta) + \theta E[c(t); H_{t-1}], & \text{if } h = 0, \\ \theta E[c; H_{t-1}], & \text{otherwise,} \end{cases}$$

139 Further, we model the time-dependent variation in the reporting probability.

140 This time dependence was modelled by introducing a parameter δ_2 , which is given by

$$\delta_2 = \begin{cases} \alpha_1, & \text{if } t = \text{period}_3, \\ \alpha_2, & \text{if } t = \text{period}_4, \\ 1, & \text{otherwise,} \end{cases}$$

141 where period_3 and period_4 represent the corresponding periods from the start of our
 142 study period to Jan 16 and from Jan 17 to Jan 22, respectively, while α_1 and α_2 scale the
 143 extent of the reporting probability (where α_1 and α_2 is expected to be smaller than 1).

144 We evenly divide the time interval before the lockdown was put in place into two
 145 periods in order to incorporate the time dependency of the reporting probability. The
 146 number of expected newly observed cases should be updated as

$$E[h(t); H_{t-1}] = \begin{cases} (1 - \theta) + q\delta\theta E[c(t); H_{t-1}], & \text{if } h_a = 0, \\ q\delta\theta E[c(t); H_{t-1}], & \text{otherwise,} \end{cases}$$

147 We assume the incidence, $h(t)$ is the result of the Binomial sampling process with the

148 expectation $E[h]$. The likelihood function for the time series of observed cases that we
149 employ to estimate the effective reproduction number and other relevant parameters is
150 given by:

$$L_1(U; c) = \prod_{t=1}^T \binom{E(h(t); H(t-1))}{c(t)} q^{c(t)} (1-q)^{E(h(t); H(t-1))-c(t)},$$

151 where U indicates parameter sets that are estimated from this likelihood.

152 Subsequently, the conditional probability of non-infection given residents in
153 Wuhan City at the time point of t_i , p_{t_i} , was assumed to follow a binomial distribution,
154 and the likelihood function is given by:

$$L_2(p_{t_i}; M_{t_i}, m_{t_i}) = \binom{M_{t_i}}{m_{t_i}} p_{t_i}^{m_{t_i}} (1-p_{t_i})^{M_{t_i}-m_{t_i}},$$

155 Where M_{t_i} and m_{t_i} is the number of government charted flight passengers and
156 non-infected passengers at the date of t_i , respectively, and p_{t_i} is the proportion of the
157 estimated non-infected population in Wuhan at the date of t_i , calculated from the $h(t)$
158 and catchment population in Wuhan City [3,13].

159 Serial interval estimates of COVID-19 were derived from previous studies of
160 COVID-19, indicating that it follows a gamma distribution with the mean and SD at 6.0
161 and 2.9 days, respectively, based on ref. [14,15]. The maximum value of the serial
162 interval was fixed at 28 days as the cumulative probability distribution of the gamma
163 distribution up to 28 days reaches 1.000.

164

165 **Infection fatality ratio**

166 Crude CFR and crude IFR is defined as the number of cumulative deaths
167 divided by the number of cumulative cases or infections at a specific point in time

168 without adjusting the time delay from illness onset or hospitalization to death. Next, we
 169 employed an integral equation model in order to estimate the real-time IFR. First, we
 170 estimated the real-time CFR as described elsewhere [16-18]. For the estimation, we
 171 employ the delay from hospitalization to death, f_s , which is assumed to be given by $f_s =$
 172 $F(s) - F(s-1)$ for $s > 0$ where $H(s)$ follows a gamma distribution with mean 10.1 days and
 173 SD 5.4 days, obtained from the available observed data [19].

$$L_3(\pi; c_t, \theta) = \prod_{t_i} \binom{t_i}{D_{t_i}} \left(\pi \frac{\sum_{t=2}^{t_i} \sum_{s=1}^{t-1} c_{t-s} f_s}{\sum_{t=1}^{t_i} c_t} \right)^{D_{t_i}} \left(1 - \pi \frac{\sum_{t=2}^{t_i} \sum_{s=1}^{t-1} c_{t-s} f_s}{\sum_{t=1}^{t_i} c_t} \right)^{\sum_{t=1}^{t_i} c_t - D_{t_i}}$$

174 where c_t represents the number of new cases with reported day t , and D_{t_i} is the number
 175 of new deaths with reported day t_i [16-18]. We assume that the cumulative number of
 176 observed deaths, D_t is the result of the binomial sampling process with probability π .
 177 Subsequently, crude IFR and time-delay adjusted IFR are calculated using the estimated
 178 π and h_t .

179 The total likelihood is calculated as $L=L_1L_2L_3$ and model parameters were
 180 estimated using a Monte Carlo Markov Chain (MCMC) method in a Bayesian
 181 framework. Posterior distributions of the model parameters were estimated based on
 182 sampling from the three Markov chains. For each chain, we drew 100,000 samples from
 183 the posterior distribution after a burn-in of 20,000 iterations. Convergence of MCMC
 184 chains were evaluated using the potential scale reduction statistic [20-21]. Estimates and
 185 95% credibility intervals for these estimates are based on the posterior probability

186 distribution of each parameter and based on the samples drawn from the posterior
187 distributions. All statistical analyses were conducted in R version 3.5.2 (R Foundation
188 for Statistical Computing, Vienna, Austria) using the ‘rstan’ package.

189

190 **Results**

191 The daily series of COVID-19 laboratory–confirmed incidence and cumulative
192 incidence in Wuhan in 2019–2020 are displayed in Figure 1. Overall, our dynamical
193 models yield a good fit to the temporal dynamics (i.e. incidence, cumulative incidence)
194 including an early exponential growth pattern in Wuhan. In incidence data, a few
195 fluctuations are evident, probably indicating that the surveillance system likely missed
196 many cases during the early transmission phase (Figure 1).

197 Our posterior estimates of basic reproduction number (R) in Wuhan City, China
198 in 2019–2020 was estimated to be 3.49 (95%CrI: 3.39–3.62). The time–dependent
199 scaling factors quantifying the extent of enhanced public health intervention on R is
200 0.99 (95%CrI: 0.95–1.00), declining R to 3.44 (95%CrI: 3.36–3.52) from January 23rd
201 to February 1st and 0.24 (95%CrI: 0.23–0.26), declining R to 0.84 (95%CrI: 0.81–0.88)
202 from February 2nd to February 11th, 2020. Other parameter estimates for the probability
203 of occurrence and reporting rate are 0.97 (95% CrI: 0.84–1.00) and 0.010 (95% CrI:
204 0.007–0.014), respectively. Moreover, the time–dependent scaling factor quantifying the
205 extent of reporting rate, α , is estimated to be 0.07 (95% CrI: 0.03–0.18) before January
206 16th and to be 0.99 (95% CrI: 0.96–1.00) from January 17th to January 22nd.

207 We conducted sensitivity analyses to examine how varying the mean serial
208 interval between 5.0 and 7.0 days affects our R estimates. R estimates are sensitive to
209 changes in the serial interval, ranging from 2.86 (95%CrI: 2.79–2.96) to 4.10

210 (95%CrI: \square 3.96–4.38).

211 The total number of estimated laboratory–confirmed cases (i.e. cumulative
212 cases) is 18967 (95% CrI: 16428–19680) while the actual numbers of reported
213 laboratory–confirmed cases during our study period is 19559 as of February 11th, 2020.
214 Moreover, we inferred the total number of COVID-19 infections (Figure S1). Our
215 results indicate that the total number of infections (i.e. cumulative infections) is
216 1906634 (95%CrI: 1373500– 2651124).

217 The Observed and posterior estimates of the cumulative number of deaths from
218 COVID-19 in Wuhan are displayed in Figure 2, and model–based posterior estimates of
219 the cumulative number of deaths is 821 (95%CrI: 751–892), while actual number of
220 reported deaths is 820. The estimated temporal variation in the death risk caused by
221 COVID-19 in Wuhan, China, 2019–2020 is shown in Figure 3 and Figure S2. Observed
222 and posterior estimates of the crude CFR in Wuhan City is presented in Figure 2A,
223 while observed and posterior estimates of time–delay adjusted CFR is shown in Figure
224 2B. Furthermore, Figure 3A and 3B illustrates time–delay no–adjusted IFR and
225 time–delay adjusted IFR, respectively.

226 The latest estimate of the crude CFR and time–delay adjusted CFR in Wuhan
227 appeared to be 4.3% (95% CrI: 3.9–5.0%) and 12.2% (95% CrI: 11.4–13.1%),
228 respectively, whereas the latest model–based posterior estimates of time–delay not
229 adjusted IFR and adjusted IFR, presented in Figure 3 C and D, are 0.04%(95% CrI:
230 0.03%–0.06%) and 0.12% (95%CrI: 0.08–0.17%), respectively, while the observed
231 crude CFR is calculated to be 4.06% (Table 1).

232

233 Discussion

234 In this study we derived estimates of the transmissibility and virulence of
235 COVID-19 in Wuhan City, China, by reconstructing the underlying transmission
236 dynamics using multiple data sources. Applying dynamic modeling, the reproduction
237 number, death risks as well as probabilities of occurrence and reporting rate were
238 estimated.

239 Our posterior estimates of basic reproduction number (R) in Wuhan City, China
240 in 2019–2020 is calculated to be 3.49 (95%CrI: 3.39–3.62). The time–dependent scaling
241 factor quantifying the extent of enhanced public health intervention on R is 0.99
242 (95%CrI: 0.95–1.00), declining R to 3.44 (95%CrI: 3.36–3.52) from January 23rd to
243 February 1st and a scaling factor at 0.24 (95%CrI: 0.23–0.26), declining R to 0.84
244 (95%CrI: 0.81–0.88) for February 2nd to February 11th, 2020. These R estimates
245 capturing the underlying transmission dynamics modify the impact of COVID-19, with
246 the total number of infections (i.e. cumulative infections) estimated at 1906634
247 (95%CrI: 1373500– 2651124) in Wuhan City, raising the proportion of infected
248 individuals to 19.1% (95%CrI: 13.7–26.5%) with a catchment population in Wuhan
249 City of 10 million people. Our estimates of mean reproduction number reached values
250 of 3.44, an estimate consistent with previous mean estimates in the range 2.2–3.8
251 derived by fitting epidemic models to the initial growth phase of the observed case
252 incidence [14,22,23]. By comparison, the R estimate for the Diamond Princess cruise
253 ship in Japan reached values as high as ~11 [24]. Further, these estimates are higher than
254 recent mean R estimates derived from the growth rates of the COVID-19 outbreaks in
255 Singapore ($R\sim 1.1$) [25] and Korea ($R\sim 1.5$) [26].

256

257 The sustained high R values in Wuhan City even after the lockdown and mobility
258 restrictions suggests that transmission continues inside the household or amplified in
259 healthcare settings [19], which is a landmark of past SARS and MERS outbreaks
260 [27-28]. Considering the potent transmissibility of COVID-19 in confined settings, as
261 illustrated by COVID-19 outbreaks aboard cruise ships, including the Diamond Princess
262 cruise ship, where the total number of secondary or tertiary infections reached 705
263 among more than 3,700 passengers as of February 28th, 2020 and also by the COVID-19
264 outbreak tied to the Shincheonji religious sect in South Korea where church members
265 appear to have infected from seven to 10 people [29-31], it is crucial to prevent
266 transmission in confined settings including hospital-based transmission by
267 strengthening infection control measures as well as transmission stemming from large
268 social gatherings.

269 Our most recent estimates of the crude CFR and time-delay adjusted CFR for
270 Wuhan city are at 4.3% (95% CrI: 3.9–5.0%) and 12.2% (95% CrI: 11.4–13.1%),
271 respectively. In contrast, our most recent crude IFR and time-delay adjusted IFR is
272 estimated to be 0.04% (95% CrI: 0.03%–0.06%) and 0.12% (95%CrI: 0.08–0.17%),
273 which is several orders of magnitude smaller than the crude CFR estimated at 4.06%
274 and another recent estimate of the infection fatality ratio at 0.66% (95%CrI: 0.39–1.33)
275 and 0.6% (95% CI: 0.2-1.3) in China [32, 33]. Several data and methodological
276 differences can explain these differences, which we list in Table S2. For instance, Verity
277 et al. conducts an age adjustment based on the data of age-stratified COVID-19 deaths
278 from mainland China, assumes a constant attack rate by age and adjusts for
279 demographic structure. Our IFR estimates will be compared with estimates emerging
280 from ongoing several mass serological studies in China (Wuhan City), Italy, Germany

281 the U.K., and New York. Yet, these serological studies should be carefully validated
282 since these are not exempt of limitations as discussed elsewhere [34, 35]. Also, these
283 findings indicate that the death risk in Wuhan is estimated to be much higher than those
284 in other areas, which is likely explained by hospital-based transmission [36]. Indeed,
285 past nosocomial outbreaks have been reported to elevate the CFR associated with
286 MERS and SARS outbreaks, where inpatients that tend to be older and affected by
287 underlying diseases have raised the CFR to values as high as 20% for a MERS outbreak
288 [37-38].

289 Public health authorities are interested in quantifying both R and CFR to
290 measure the transmission potential and virulence of an infectious disease, especially
291 when emerging/re-emerging epidemics occur in order to decide the intensity of the
292 public health response. In the context of a substantial fraction of unobserved infections
293 due to COVID-19, R estimates derived from the trajectory of infections and the IFR are
294 more realistic indicators compared to estimates derived from observed cases alone [18,
295 39-40].

296 Our analysis also revealed a high probability of occurrence and quite low
297 reporting probabilities in Wuhan City. High probability of occurrence in the above
298 equation suggests that zero observed cases at some point is not due to the absence of
299 those infected, but more likely due to a low reporting rate. A very low reporting
300 probability suggests that it is difficult to diagnose COVID-19 cases or a breakdown in
301 medical care delivery. Moreover, we also identified a remarkable change in the
302 reporting rate, estimated to be 14-fold lower in the 1st period (–Jan 16th, 2020) and
303 about the same during the 2nd period (January 17th – 22nd, 2020), relative to that
304 estimated after January 23rd 2020.

305

306 Our results are not free from the limitations. First, our methodology aims to capture the
307 underlying transmission dynamics using multiple data sources. By implementing mass
308 screening in certain populations is a useful approach to ascertain the real proportion of
309 those infected and a way of adding credibility to the estimated values. Second, it is
310 worth noting that the data of Japanese evacuees from Wuhan employed in our analysis
311 is not a random sample from the Wuhan catchment population. Indeed, it also plausible
312 that their risk of infection in this sample is not as high as that of local residents in
313 Wuhan, underestimating the fatality risk. Third, given the likely under-ascertainment of
314 cases, there may also exist unreported deaths, and this might underestimate the death
315 risk. Fourth, case fatality ratio (CFR) varies with age, gender, presence or absence of
316 comorbidities, race, whether the healthcare system is overloaded or not, and other
317 factors such as poverty risk, infant mortality risk, and the cumulative morbidity ratio
318 [41-45]. As CFR is influence by reporting rate and ascertainment bias, subgroup
319 analysis of IFR based on individual-level data is essential to capture the overall disease
320 burden of COVID-19.

321

322 **Conclusion**

323 In summary, we have estimated key epidemiological parameters of the
324 transmissibility and virulence of COVID-19 in Wuhan, China, January-February, 2020
325 using an ecological modelling approach and several epidemiological datasets. The
326 power of our approach lies in the ability to infer epidemiological parameters with
327 quantified uncertainty from partial observations collected by surveillance systems.

328

329 **List of abbreviations**

330 CFR: Case fatality ratio, IFR: Infection Fatality ratio, SARS: Severe Acute Respiratory

331 Syndrome, MERS: Middle East Respiratory Syndrome

332

333 **Additional files**

334 **Additional file 1: Table S1.** Information related to Japanese evacuees from Wuhan City

335 on board government-chartered flights. **Table S2.** Main differences between our study

336 and previous study.

337 **Additional file 2: Fig. S1. Observed daily new cases and posterior estimates of the**

338 **daily new infections of the COVID-19 in Wuhan, China, 2019–2020.**

339 Observed daily new cases and posterior estimates of infections of the COVID-19 are

340 presented. Observed data are presented in the dot, while dashed line indicates 50

341 percentile, and areas surrounded by light grey and deep grey indicates 95% and 50%

342 credible intervals (CrI) for posterior estimates, respectively. Epidemic day 1

343 corresponds to the day that starts at January 1st, 2020.

344

345 **Additional file 3: Fig. S2. Temporal variation of the case fatality risks caused by**

346 **COVID-19 in Wuhan, China, 2019–2020.**

347 (A) Observed and posterior estimates of crude case fatality ratio in Wuhan City, (B)
348 Observed crude case fatality ratio and posterior estimates of time–delay adjusted CFR
349 in Wuhan City. This figure is submitted to the ref [19]. The purpose of the study is to
350 compare the case fatality ration (CFR. Not IFR) in three different areas (Wuhan City, in
351 Hubei Province excluding Wuhan City and in China excluding Hubei Province) to
352 interpret the current severity of the epidemic in China, and the purpose is different from
353 this study.

354

355

356 **Declarations**

357 **Ethics approval and consent to participate**

358 Not applicable.

359 **Consent for publication**

360 Not applicable.

361 **Availability of data and materials**

362 The present study relies on published data and access information to essential
363 components of the data are available from the corresponding author.

364 **Competing interests**

365 The authors declare that they have no competing interests.

366

367 **Funding**

368 KM acknowledges support from the Japan Society for the Promotion of Science (JSPS)
369 KAKENHI (Grant Number 18K17368 and 20H03940) and from the Leading Initiative
370 for Excellent Young Researchers from the Ministry of Education, Culture, Sport,
371 Science & Technology of Japan. KK acknowledges support from the JSPS KAKENHI
372 Grant Number 18K19336 and 19H05330. GC acknowledges support from NSF grant
373 1414374 as part of the joint NSF–NIH–USDA Ecology and Evolution of Infectious
374 Diseases program.

375 **Authors' contributions**

376 KM and GC conceived the early study idea. KM and KK built the model. KM
377 implemented statistical analysis and wrote the first full draft. GC advised on and helped
378 shape the research. All authors contributed to the interpretation of the results and edited
379 and commented on several earlier versions of the manuscript. All authors read and
380 approved the final manuscript.

381 **Acknowledgements**

382 Not applicable.
383

384 **REFERENCES**

- 385 1. Jon Cohen. **Mining coronavirus genomes for clues to the outbreak's origins.**
386 **Science.** Jan 31, 2020.

- 387 <https://www.sciencemag.org/news/2020/01/mining-coronavirus-genomes-clues->
388 [outbreak-s-origins](https://www.sciencemag.org/news/2020/01/mining-coronavirus-genomes-clues-). Accessed, Feb 3rd, 2020
- 389 2. World Health Organization (WHO). Novel Coronavirus (2019-nCoV) situation
390 reports. Available from:
391 <https://www.who.int/emergencies/diseases/novel-coronavirus-2019/situation-rep>
392 [orts](https://www.who.int/emergencies/diseases/novel-coronavirus-2019/situation-rep) Accessed, [cited 2020 May 10th]
- 393 3. The State Council, The People’s Republic of China. [cited 2020 May 10th].
394 <http://www.gov.cn/>
- 395 4. Nishiura H, Jung SM, Linton NM, Kinoshita R, Yang Y, Hayashi K, et al. **The**
396 **Extent of Transmission of Novel Coronavirus in Wuhan, China, 2020.** *J Clin*
397 *Med.* 2020; 9(2); 330
- 398 5. Wu JT, Leung K, Leung GM. **Nowcasting and forecasting the potential**
399 **domestic and international spread of the 2019-nCoV outbreak originating**
400 **in Wuhan, China: a modelling study.** *Lancet.* 2020. pii:
401 S0140-6736(20)30260-9. doi: 10.1016/S0140-6736(20)30260-9.
- 402 6. Linton NM, Kobayashi T, Yang Y, Hayashi K, Akhmetzhanov AR, Jung SM, et
403 al. **Epidemiological characteristics of novel coronavirus infection: A**

- 404 **statistical analysis of publicly available case data.** *medRxiv*
- 405 2020.01.26.20018754; doi: <https://doi.org/10.1101/2020.01.26.20018754>
- 406 7. Health Commission of Hubei Province, China. [cited 2020 Feb 7th].
- 407 <http://wjw.hubei.gov.cn/>
- 408 8. Health Commission of Wuhan City, Hubei Province, China [cited 2020 Feb 7th]
- 409 <http://wjw.hubei.gov.cn/>
- 410 9. Clinical guideline for COVID-19, version 5. The State Council, The People's
- 411 Republic of China. Available from
- 412 [http://www.gov.cn/zhengce/zhengceku/2020-02/05/5474791/files/de44557832a](http://www.gov.cn/zhengce/zhengceku/2020-02/05/5474791/files/de44557832ad4be1929091dcbcfca891.pdf)
- 413 [d4be1929091dcbcfca891.pdf](http://www.gov.cn/zhengce/zhengceku/2020-02/05/5474791/files/de44557832ad4be1929091dcbcfca891.pdf) [Accessed Feb 29th, 2020][in Chinese]
- 414 10. Ministry of Health, Labour and Welfare, Japan.
- 415 <https://www.mhlw.go.jp/index.html> [in Japanese]
- 416 11. 2020 Hubei lockdowns, Wikipedia.
- 417 https://en.wikipedia.org/wiki/2020_Hubei_lockdowns
- 418 12. Li R,a Weiskittel AR,a Kershaw Jr, JA. **Modeling annualized occurrence,**
- 419 **frequency, and composition of ingrowth using mixed-effects zero-inflated**
- 420 **models and permanent plots in the Acadian Forest Region of North**
- 421 **America.** *Can J For Res.* 2011; 41:2077–2089

- 422 13. Northeastern University. Laboratory for the Modeling of Biological and Socio -
423 Technical Systems, 2020. Available online: [https://www.mobs -](https://www.mobs-lab.org/2019ncov.html)
424 [lab.org/2019ncov.html](https://www.mobs-lab.org/2019ncov.html) [accessed on January 22nd, 2020).
- 425 14. Li Q, Guan X, et. al. **Early Transmission Dynamics in Wuhan, China, of**
426 **Novel Coronavirus–Infected Pneumonia.** *N Engl J Med.* 2020 Jan 29. DOI:
427 10.1056/NEJMoa2001316 Available at:
428 <https://www.nejm.org/doi/full/10.1056/NEJMoa2001316>
- 429 15. Nishiura H, Linton NM, Akhmetzhanov AR. *Int J Infect Dis.* 2020
430 Apr;93:284-286. doi: 10.1016/j.ijid.2020.02.060
- 431 16. Ghani AC, Donnelly CA, Cox DR, Griffin JT, Fraser C, Lam TH, et al.
432 **Methods for estimating the case fatality ratio for a novel, emerging**
433 **infectious disease.** *Am J Epidemiol.* 2005; 162: 479-486
- 434 17. Nishiura H, Klinkenberg D, Roberts M, Heesterbeek JA. **Early epidemiological**
435 **assessment of the virulence of emerging infectious diseases: a case study of**
436 **an influenza pandemic.** *PLoS One.* 2009;4(8):e6852. doi:
437 10.1371/journal.pone.0006852.
- 438 18. Tsuzuki S, Lee H, Miura F, Chan YH, Jung SM, Akhmetzhanov AR, Nishiura H.
439 **Dynamics of the pneumonic plague epidemic in Madagascar, August to**

- 440 **October 2017. *Euro Surveill.* 2017;22(46). doi:**
- 441 10.2807/1560-7917.ES.2017.22.46.17-00710.
- 442 19. Mizumoto K, Chowell G. **Estimating the risk of 2019 Novel Coronavirus**
- 443 **death during the course of the outbreak in China, 2020. *Emerg Infect Dis.***
- 444 2020; 26.
- 445 20. Gamerman, D. & Lopes, H. F. **Markov Chain Monte Carlo: Stochastic**
- 446 **Simulation for Bayesian Inference.** 2nd edn (Chapman & Hall/CRC, 2006).
- 447 21. Gelman, A. & Rubin, D. B. **Inference from iterative simulation using**
- 448 **multiple sequences. *Stat Sci* 7:457-472, doi:10.1214/ss/1177011136 (1992).**
- 449 22. Read JM, Bridgen JR, Cummings DA, Ho A, Jewell CP. **Novel coronavirus**
- 450 **2019-nCoV: early estimation of epidemiological parameters and epidemic**
- 451 **predictions. *medRxiv.* doi: <https://doi.org/10.1101/2020.01.23.20018549>**
- 452 23. Imai N, Cori A, Dorigatti I, Baguelin M, Donnelly CA, Riley S, Ferguson NM.
- 453 **Report 3: Transmissibility of 2019-nCoV.**
- 454 <https://www.imperial.ac.uk/media/imperial-college/medicine/sph/ide/gida-fello>
- 455 [wships/Imperial-2019-nCoV-transmissibility.pdf](https://www.imperial.ac.uk/media/imperial-college/medicine/sph/ide/gida-fellowships/Imperial-2019-nCoV-transmissibility.pdf)

- 456 24. Mizumoto K, Chowell G. **Transmission potential of the novel coronavirus**
457 **(COVID-19) onboard the Diamond Princess Cruises Ship, 2020.** *Infect Dis*
458 *Model.* 2020. 264-270
- 459 25. Tariq A, Lee Y, Roosa K, Blumberg S, Yan P, Ma S, Chowell G. **Real-time**
460 **monitoring the transmission potential of COVID-19 in Singapore, February**
461 **2020.** *medRxiv.* doi: <https://doi.org/10.1101/2020.02.21.20026435>
- 462 26. Shim E, Tariq A, Choi W, Lee Y, Chowell G. **Transmission potential of**
463 **COVID-19 in South Korea.** *medRxiv.*
464 doi:<https://doi.org/10.1101/2020.02.27.20028829>
- 465 27. Chowell G, Abdirizak F, Lee S, Lee J, Jung E, Nishiura H, Viboud C.
466 **Transmission characteristics of MERS and SARS in the healthcare setting:**
467 **a comparative study.** *BMC Med.* 2015;**13**:210. doi:
468 10.1186/s12916-015-0450-0.
- 469 28. Abdirizak F, Lewis R, Chowell G. **Evaluating the potential impact of targeted**
470 **vaccination strategies against severe acute respiratory syndrome**
471 **coronavirus (SARS-CoV) and Middle East respiratory syndrome**
472 **coronavirus (MERS-CoV) outbreaks in the healthcare setting.** *Theor Biol*
473 *Med Model.* 2019;**16**(1):16. doi: 10.1186/s12976-019-0112-6.

- 474 29. Blake Essig, Brent Swails, Yoko Wakatsuki and Ben Westcott, CNN. **Top**
475 **Japanese government adviser says Diamond Princess quarantine was**
476 **flawed.** Updated 0708 GMT (1508 HKT) February 27, 2020.
477 <https://edition.cnn.com/2020/02/27/asia/japan-diamond-princess-quarantine-cre>
478 [w-intl-hnk/index.html](https://www.intl-hnk.com/index.html)
- 479 30. Da-hae P, Dam-eun S, Jae-gu K. HANKYOREH. **The reasons why**
480 **transmission is so prevalent among Shincheonji members.** Mar 2, 2020.
481 http://english.hani.co.kr/arti/english_edition/e_national/930749.html [Accessed
482 Mar/10, 2020]
- 483 31. Mizumoto K, Kagaya K, Zarebski A, Chowell G. **Estimating the**
484 **Asymptomatic Proportion of 2019 Novel Coronavirus onboard the Princess**
485 **Cruises Ship, 2020.** *Euro Surveill.* 2020; 25.
- 486 32. Verity R, Okell LC, Dorigatti I, Winskill P, Whittaker C, Imai N, et al.
487 **Estimates of the severity of coronavirus disease 2019: a model-based**
488 **analysis.** *Lancet Infect Dis.* 2020. pii: S1473-3099(20)30243-7.
- 489 33. Russell TW, Hellewell J, Jarvis CI, et al. **Estimating the Infection and Case**
490 **Fatality Ratio for Coronavirus Disease (COVID-19) Using Age-Adjusted**
491 **Data From the Outbreak on the Diamond Princess Cruise Ship, February**

- 492 **2020. *Euro Surveill.* 2020; 25(12): 2000256. doi:**
493 10.2807/1560-7917.ES.2020.25.12.2000256.
- 494 34. Wu X, Fu B, Chen L, Feng Y. **Serological tests facilitate identification of**
495 **asymptomatic SARS-CoV-2 infection in Wuhan, China.** *Journal of Medical*
496 *Virology.* <https://doi.org/10.1002/jmv.25904>
- 497 35. Giugliano F. **Mass Coronavirus Antibody Tests Have Serious Limits.**
498 *Bloomberg Opinion.* April 24, 2020. [Accessed on May 30th, 2020]
- 499 36. Wang D, Hu B, Hu C, Zhu F, Liu X, Zhang J, et al. **Clinical Characteristics of**
500 **138 Hospitalized Patients With 2019 Novel Coronavirus-Infected**
501 **Pneumonia in Wuhan, China.** *JAMA.* 2020. doi: 10.1001/jama.2020.1585.
- 502 37. Mizumoto K, Endo A, Chowell G, Miyamatsu Y, Saitoh M, Nishiura H.
503 **Real-time characterization of risks of death associated with the Middle East**
504 **respiratory syndrome (MERS) in the Republic of Korea, 2015.** *BMC Med.*
505 2015;**13**:228. doi: 10.1186/s12916-015-0468-3.
- 506 38. Mizumoto K, Saitoh M, Chowell G, Miyamatsu Y, Nishiura H. **Estimating the**
507 **risk of Middle East respiratory syndrome (MERS) death during the course**
508 **of the outbreak in the Republic of Korea, 2015.** *Int J Infect Dis.* 2015;**39**:7-9.
509 doi: 10.1016/j.ijid.2015.08.005.

- 510 39. J.Y. Wong, P. Wu, H. Nishiura, E. Goldstein, E.H. Lau, L. Yang, et al. **Infection**
511 **fatality risk of the pandemic A(H1N1)2009 virus in Hong Kong.** *Am J*
512 *Epidemiol.* 2013;**177 (8)**:pp. 834-840
- 513 40. Presanis AM, De Angelis D; New York City Swine Flu Investigation Team,
514 Hagy A, Reed C, Riley S, Cooper BS, et al. **The severity of pandemic H1N1**
515 **influenza in the United States, from April to July 2009: a Bayesian analysis.**
516 *PLoS Med.* 2009;**6(12)**:e1000207.
- 517 41. The Guardian. **Black people four times more likely to die from Covid-19,**
518 **ONS finds.**
519 <https://www.theguardian.com/world/2020/may/07/black-people-four-times-more>
520 [-likely-to-die-from-covid-19-ons-finds](#) [accessed May 29, 2020]
- 521 42. Mizumoto K, Dahal S, Chowell G. **Spatial variability in the risk of death**
522 **from COVID-19 in 20 regions of Italy.** *medRxiv.* 2020.04.01.20049668.
- 523 43. Shim E, Mizumoto K, Choi W, et al. **Estimating the risk of COVID-19 death**
524 **during the course of the outbreak in Korea, February- May, 2020.** *medRxiv.*
525 2020.03.30.20048264.

- 526 44. Dahal S, Mizumoto K, Chowell G. **Investigating spatial variability in**
527 **COVID-19 pandemic severity across 19 geographic areas, Spain, 2020.**
528 *medRxiv*. 2020.04.14.20065524.
- 529 45. Undurraga EA, Chowell G, Mizumoto K. **Case fatality risk by age from**
530 **COVID-19 in a high testing setting in Latin America: Chile, March-May,**
531 **2020.** *medRxiv*. 2020.05.25.20112904.
- 532
- 533

534 **Figures**

535 **Figure 1. Observed and posterior estimates of the daily new cases and**

536 **cumulative cases of the COVID-19 cases in Wuhan, China, 2019–2020**

537 Observed and posterior estimates of laboratory–confirmed reported cases (A) and

538 cumulative reported cases (B) are presented.

539 Observed data are presented in the dot, while dashed line indicates 50 percentile, and

540 areas surrounded by light grey and deep grey indicates 95% and 50% credible intervals

541 (CrI) for posterior estimates, respectively. Epidemic day 1 corresponds to the day that

542 starts at January 1st, 2020.

543

544 **Figure 2. Observed and posterior estimates of the cumulative deaths of the**

545 **COVID-19 in Wuhan, China, 2019–2020**

546 Observed and posterior estimates of the cumulative deaths of the COVID-19 in Wuhan

547 is presented. Observed data are presented in the dot, while dashed line indicates 50

548 percentile, and areas surrounded by light grey and deep grey indicates 95% and 50%

549 credible intervals (CrI) for posterior estimates, respectively. Epidemic day 1

550 corresponds to the day that starts at January 1st, 2020.

551

552 **Figure 3. Temporal variation of the infection fatality risks caused by COVID-19 in**

553 **Wuhan, China, 2019–2020**

554

555 (A) Posterior estimates of crude infection fatality ratio in Wuhan City. (B) Posterior
556 estimates of time–delay adjusted infection fatality ratio in Wuhan City.
557 Black dots shows observed data, and light and dark indicates 95% and 50% credible
558 intervals for posterior estimates, respectively. Epidemic day 1 corresponds to the day
559 that starts at January 1st, 2020.
560

561 **Tables**

562 Table 1 – Death risk by COVID-19 in Wuhan City, China, 2020 (As of
563 February 12, 2020)

Death Risk	Latest estimate	Range of median estimates
Crude CFR (Observed)	4.06%	2.0 – 9.0%
Crude CFR (Estimated)	4.3% (95%CrI [‡] : 3.9 – 5.0%)	3.4 – 7.1%
Time delay adjusted CFR	12.2% (95%CrI: 11.4 – 13.1%)	4.0 – 34.5%
Crud IFR	0.04% (95%CrI: 0.03 – 0.06%)	0.02 – 0.07%
Time delay adjusted IFR	0.12% (95%CrI: 0.08 – 0.17%)	0.03 – 0.33%

564 CrI: Credibility intervals, CFR: Case fatality ratio, IFR: Infection fatality
565 ratio

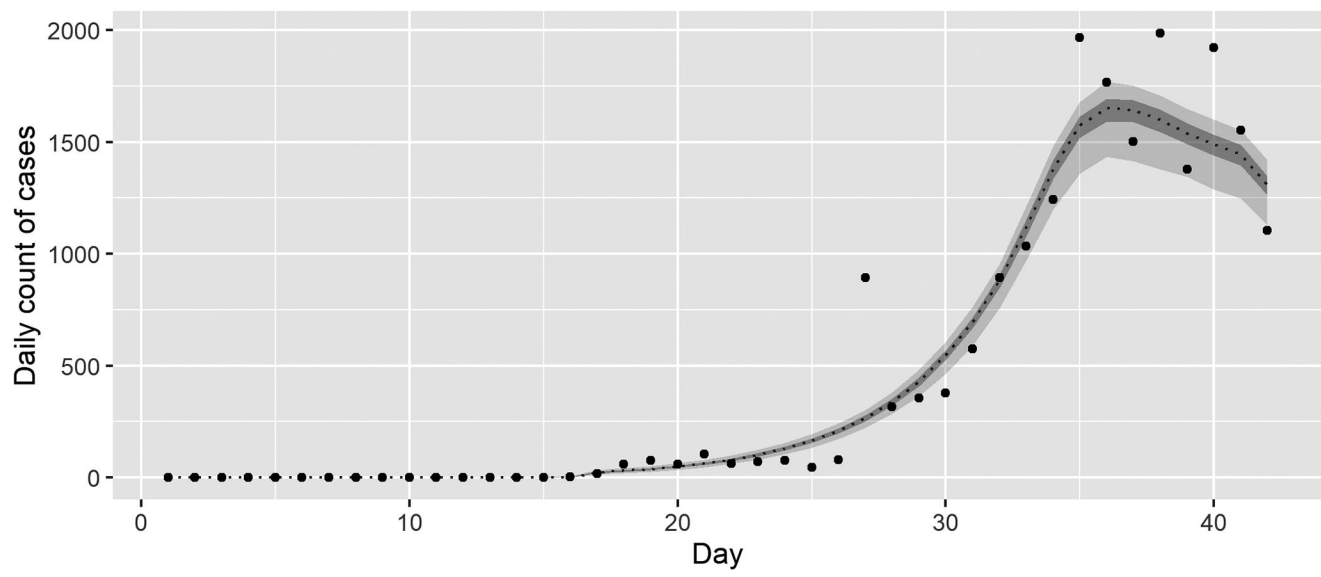
566 [‡]Upper and lower 95% credibility interval

567

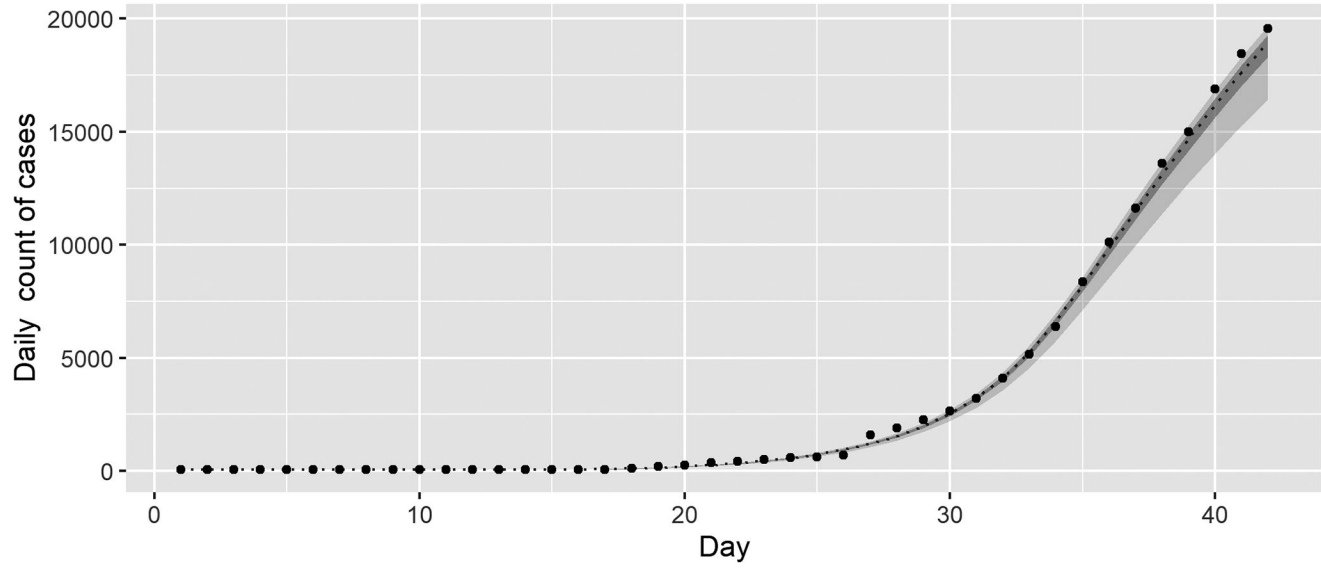
568

569

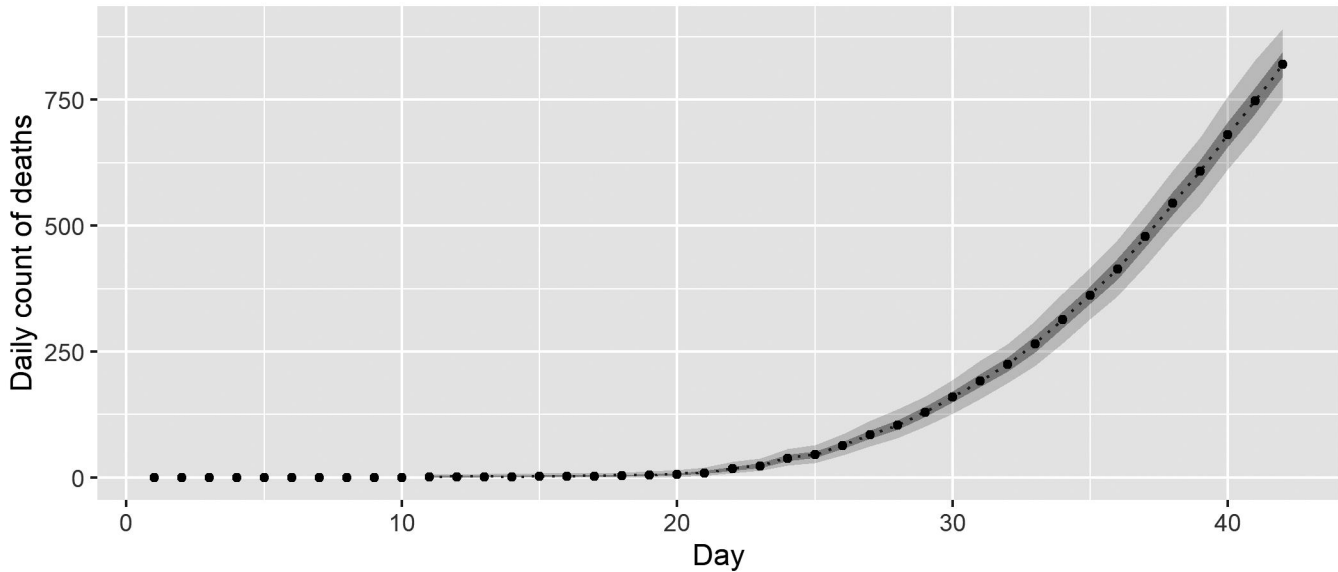
A Observed and estimated number of reported cases
Wuhan



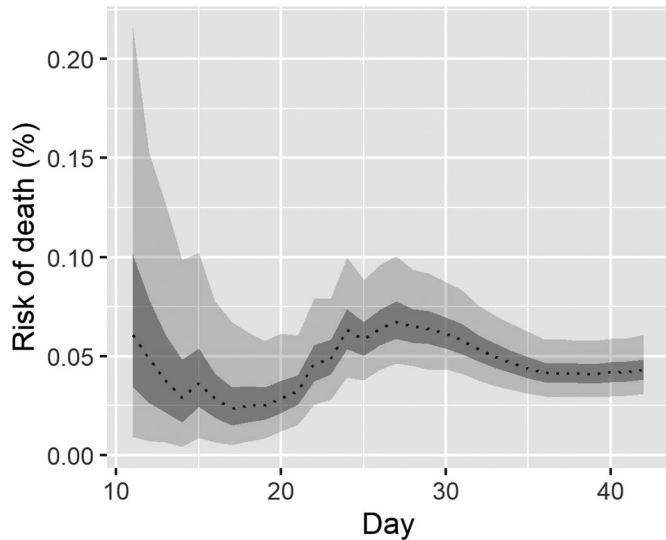
B Observed and estimated number of cumulative reported cases
Wuhan



Observed and estimated number of reported cumulative death
Wuhan



A Infection fatality ratio
Crude
Wuhan



B Infection fatality ratio
Time-delay adjusted
Wuhan

